Applied Chemical Engineering (2025) Volume 8 Issue 4 ISSN: 2578-2010 (O)
doi: 10.59429/ace.v8i4.5726

ORIGINAL RESEARCH ARTICLE

Photopolymer resin formulation and surface modification for enhanced coating applications in SLA-Printed devices

Sanan Thaer Abdalwahab [1], Ala'a D. Noor[2], Haider Falih Shamikh Al-Saedi[3] , Mohannad Mohammed[4] , Nour Sabah Kadhim[5] , Nawal Fattah Naji[6] , Imad Ibrahim Dawood[7] , Hiba Alaa Mohammed[8,*]

[1]*Department of Medicinal Chemistry, College of Pharmacy, Al-Turath University, Baghdad,10013, Iraq*

[2]*Department of Pharmaceutics, College of Pharmacy, Al Farahidi University, Baghdad, 10111,Iraq*

[3] *Department of pharmaceutics , Faculty of pharmacy,University of Al-Ameed, Karbala Governorate, 56001,Iraq*

[4] *Department of Mathematics, Warka University College, Basrah,110073,Iraq*

[5] *Department of sciences, Al-Manara College For Medical Sciences,University of Manara, Maysan, 62010,Iraq*

[6] *Department of Medical Physics, Al-Hadi University College, Baghdad, 10011, Iraq*

[7] *Faculty of Education for Humanities, Mazaya University College,Dhi Qar, 21974,Iraq*

[8]*Department of Medical Laboratory Techniques, College of Health and Medical Techniques. Al-Bayan University, Baghdad,6111, Iraq*

***Corresponding author:** Hiba Alaa Mohammed, hiba.al@albayan.edu.iq

ARTICLE INFO

Received: 8 August 2025
Accepted: 28 September 2025
Available online: 09 October 2025

ABSTRACT

Stereolithography (SLA) has emerged as a superior additive manufacturing technique compared to Fused Deposition Modeling (FDM), offering smoother surface finishes and higher dimensional accuracy. However, conventional SLA resins remain limited by brittleness, poor thermal stability, and weak coating adhesion. In this study, a hybrid photopolymer resin incorporating nano-silica fillers (0.5–2.0 wt%) and functional oligomers was formulated, alongside plasma–silanization surface treatments, to enhance coating performance of SLA-printed parts. Mechanical testing showed a peak improvement at 1.0 wt% nano-silica, where tensile strength increased by 35.9% (from 32.5 MPa to 44.2 MPa), Young's modulus by 36.2% (870 MPa to 1185 MPa), and flexural strength by 29.9% (58.9 MPa to 76.5 MPa). Shore D hardness rose from 78 to 84, while thermal analysis revealed an upward shift in glass transition temperature from 64.2 °C to 70.5 °C and degradation onset temperature from 281 °C to 301 °C. Surface wettability improved significantly, with water contact angle reduced from 89.3° to 54.7°, raising surface energy from 32.4 to 51.1 mN/m. Coating adhesion (ASTM D3359) improved from grade 3B to 5B, and wear resistance increased by 40% (wear index reduced from 0.125 to 0.075 mg/cycle). These results validate the dual-pathway approach of resin reinforcement and post-print surface modification, enabling SLA-printed parts to overcome typical FDM limitations of poor surface fidelity and weak interfacial bonding. The developed system demonstrates strong potential for high-performance coatings in biomedical, optical, and microfluidic device applications.

Keywords: Photopolymer Resin; Stereolithography (SLA); additive manufacturing; surface modification; coating applications; uv-curable resins; functional additives; nano-silica reinforcement; 3D printing materials

1. Introduction

The emergence of stereolithography (SLA) as a leading additive manufacturing (AM) technique has revolutionized the fabrication of high-resolution components, enabling the production of microscale devices with intricate geometries and smooth surface finishes [1-3]. SLA utilizes photopolymer resins that cure layer-by-layer under ultraviolet (UV) light, offering distinct advantages in terms of dimensional accuracy, surface fidelity, and material versatility compared to traditional Fused Deposition Modeling (FDM) or Selective Laser Sintering (SLS) techniques. As this technology becomes increasingly prevalent in biomedical, optical, microfluidic, and surface coating applications, the demands placed on the functional performance of the printed parts have grown substantially [4-7]. Conventional SLA resins, often composed of acrylate or methacrylate monomers, exhibit several performance limitations, including poor thermal resistance, mechanical brittleness, low chemical stability, and suboptimal surface interaction when subjected to post-processing or coating protocols [8-12]. Moreover, the inherent brittleness and limited interfacial adhesion of SLA-printed parts restrict their utility in real-world environments where mechanical integrity and surface functionality are critical. Recent state-of-the-art developments have begun to address these deficiencies by introducing novel resin chemistries such as epoxy-acrylates, thiol-ene systems, and oligomeric hybrids, alongside the incorporation of fillers like silica nanoparticles, ceramic microparticles, or carbon-based additives to improve structural integrity [13-17]. Additionally, advancements in surface modification strategies including plasma activation, silanization, UV post-curing, and graft polymerization have demonstrated the potential to significantly alter the surface properties of SLA prints, thereby enhancing their compatibility with paints, coatings, or biomedical agents. Nonetheless, despite promising progress, there remains a considerable gap in achieving a unified approach that concurrently addresses both the bulk mechanical performance and surface characteristics of SLA-fabricated components. Existing studies often focus exclusively on resin formulation or post-print surface treatment in isolation, lacking a comprehensive strategy that integrates these two domains to produce SLA parts tailored for high-performance coating applications.

While SLA has gained prominence due to its ability to deliver high-resolution, smooth-surfaced components, it is important to contrast it with the widely used Fused Deposition Modeling (FDM). FDM, which extrudes thermoplastic filaments such as PLA or ABS, is cost-effective and widely accessible; however, it suffers from visible layer lines, anisotropic mechanical properties, and poor surface finish, making it less suitable for applications demanding precise microfeatures or coating adhesion. For instance, the average surface roughness (Ra) of FDM-printed parts typically ranges from 10–25 µm, compared to <2 µm achievable with SLA. Moreover, FDM parts often require extensive post-processing (e.g., sanding, acetone vapor smoothing) to improve surface quality, whereas SLA prints inherently produce superior surface fidelity [18-22]. Selective Laser Sintering (SLS) provides stronger mechanical integrity than FDM and SLA, but its powder-based process results in rougher surfaces and higher equipment costs. Thus, SLA occupies a unique position: combining higher resolution and smoother finishes than FDM and SLS, but with intrinsic weaknesses in resin brittleness, thermal stability, and surface adhesion. These shortcomings motivate the present study, which integrates nano-silica reinforcement with plasma–silanization surface treatments to overcome SLA's limitations and extend its competitiveness into functional coating applications [23-26].

In this context, the present study introduces a dual-pathway strategy that aims to formulate a photopolymer resin with embedded functional additives while simultaneously optimizing surface properties through post-fabrication modification techniques. The novelty of this work lies in its holistic approach: rather than treating resin formulation and surface treatment as separate enhancements, this research integrates both dimensions to produce a synergistic effect on coating performance and device durability. Specifically, the resin system developed in this study incorporates UV-curable oligomers, reactive diluents, and nano-silica particles, designed to increase crosslinking density and reduce polymer shrinkage while improving mechanical robustness and thermal stability. Parallel to this, the SLA-printed surfaces undergo systematic surface modification, employing plasma treatment to activate polar groups, followed by silane coupling agents to improve hydrophilic/hydrophobic balance and chemical reactivity. Such treatments aim to optimize the surface energy of printed substrates, enhancing wettability, interlayer adhesion, and compatibility with subsequent coatings or surface-functionalized materials. The objective of this research is thus twofold: (1) to develop a tailored photopolymer resin system that ensures improved mechanical and thermal performance, and (2) to implement and evaluate surface modification strategies that elevate coating adhesion, surface smoothness, and chemical resistance. The methodology is based on experimental design, where resin formulations are synthesized under controlled conditions, followed by SLA printing of test samples. The printed parts are then subjected to a series of surface treatments and characterized using Fourier-transform infrared spectroscopy (FTIR) for chemical group identification, contact angle goniometry for surface energy assessment, atomic force microscopy (AFM) and profilometry for topographical evaluation, and mechanical testing for tensile and flexural strength. Though complete results are in progress, preliminary characterization suggests that the combined effect of functional resin chemistry and surface modification significantly outperforms conventional SLA materials in terms of coating adhesion and surface functionality.

This integrated approach is expected to serve as a practical framework for enhancing SLA-printed devices used in critical applications such as biomedical coatings, optoelectronic interfaces, and microfluidic surface channels, where material performance and surface reliability are non-negotiable. Furthermore, this research bridges the current gap in SLA additive manufacturing by offering a material-process co-optimization model addressing not just how a material is printed, but how its formulation and surface conditioning can be tailored for a given end-use scenario. The novelty also extends to the selection and synergistic combination of nano-silica fillers with plasma-enhanced silanization, a pairing not extensively documented in SLA-specific literature. By anchoring surface chemistry enhancements directly to the modified polymer backbone, the method enhances coating adhesion without sacrificing mechanical strength a trade-off commonly encountered in conventional SLA surface treatments. Structurally, this paper is organized as follows: Section 2 presents a detailed overview of materials and methods, including resin synthesis protocols, 3D printing parameters, and surface treatment techniques. Section 3 outlines the characterization procedures and performance metrics used to evaluate both bulk and surface properties. Section 4 discusses the preliminary results and their implications, comparing them with existing literature benchmarks. Finally, Section 5 concludes with key takeaways, limitations, and directions for future research. Collectively, this study contributes to the advancement of materials engineering in additive manufacturing by offering a scalable and effective solution to enhance both the intrinsic and extrinsic properties of SLA-printed parts for coating-oriented applications.

2. Materials and methods

In this study, all test specimens and functional devices were fabricated using the ELEGOO Saturn 4 Ultra Resin Fast 3D Printer, an advanced MSLA (Masked Stereolithography Apparatus) system that operates at a wavelength of 405 nm and offers 12K high-resolution monochrome LCD projection with a build volume of 218.88 mm × 122.88 mm × 250 mm. The printer's fast-curing technology, with an average exposure time

of 1.5–2.0 seconds per layer and a minimum layer thickness of 0.01 mm, enabled high-precision prototyping and the controlled production of uniform sample batches. The resin formulations were developed in-house using a hybrid system comprising urethane dimethacrylate (UDMA) as the base oligomer, combined with triethylene glycol dimethacrylate (TEGDMA) as the reactive diluent to adjust viscosity and crosslinking behavior. Nano-silica (SiO_2) particles with an average diameter of 20–30 nm were used as fillers in concentrations of 0.5 wt%, 1.0 wt%, and 2.0 wt% to assess their influence on mechanical, thermal, and surface properties. Photo-initiators such as diphenyl(2,4,6-trimethylbenzoyl)phosphine oxide (TPO) and UV absorbers were added at 1–2 wt% to ensure optimal photopolymerization under the 405 nm LED light source. The resin mixtures were homogenized using a dual-mode magnetic stirrer and ultrasonic probe sonicator for 30 minutes to achieve uniform filler dispersion. All resin formulations were filtered through a 0.45 μm nylon membrane to remove agglomerates and degassed under vacuum for 15 minutes prior to printing. Standard ASTM D638 Type V tensile specimens were printed for mechanical testing, while ASTM D790-compliant rectangular bars were used for flexural analysis. Disc-shaped samples (diameter: 25 mm, thickness: 2 mm) were fabricated for contact angle and FTIR characterization. The printing parameters were fixed across all batches to ensure comparability, with a base exposure of 30 seconds, layer exposure of 2.0 seconds, bottom layer count of 5, and a lifting speed of 3 mm/s. Following the printing process, all specimens underwent post-curing under a 405 nm UV LED chamber for 15 minutes at 60°C to complete the crosslinking reaction and stabilize mechanical properties.

Surface modification was performed using a three-step post-treatment procedure. First, plasma surface activation was conducted using an oxygen plasma cleaner (Harrick Plasma PDC-002) at a power setting of 30 W for 5 minutes under low vacuum conditions (0.5 mbar) to introduce polar functional groups and increase surface energy. This treatment promotes the formation of hydroxyl and carboxyl functionalities on the polymer surface, which serve as anchoring points for subsequent silanization. Second, the plasma-treated samples were immersed in a 2 vol% solution of 3-aminopropyltriethoxysilane (APTES) prepared in ethanol for 30 minutes, then rinsed in deionized water and dried at 60°C. Silanization facilitates the formation of a covalent siloxane network, enhancing surface hydrophilicity and chemical reactivity. Lastly, UV post-curing was reapplied for 10 minutes to consolidate the silane coating and improve interfacial adhesion. Surface energy was quantified using static contact angle measurements following ASTM D7334, using deionized water and diiodomethane as probe liquids. Each sample was measured at three distinct surface locations, and the Owens–Wendt method was used to calculate polar and dispersive components of the total surface energy. Topographical features were analyzed using atomic force microscopy (AFM, Bruker Dimension Icon) and surface profilometry (Mitutoyo SJ-410), with roughness parameters Ra and Rq reported over a scan area of 5 μm × 5 μm. FTIR spectroscopy (Nicolet iS5, Thermo Fisher) was employed in ATR mode to verify chemical changes in the surface groups pre- and post-treatment across the 4000–5000 cm^{-1} spectral range. Thermogravimetric analysis (TGA) and differential scanning calorimetry (DSC) were conducted following ASTM E1131 and ASTM D3418, respectively, to determine thermal stability and glass transition temperatures (Tg) of the printed composites.

Mechanical properties were assessed using a universal testing machine (Instron 3366) with a 10 kN load cell. Tensile tests were carried out at a crosshead speed of 5 mm/min per ASTM D638 standards. The ultimate tensile strength (UTS), Young's modulus, and elongation-at-break were recorded as average values from five replicates per formulation. Flexural strength and modulus were measured via three-point bending tests under ASTM D790 conditions with a support span of 50 mm and a loading speed of 1.3 mm/min. Hardness testing was conducted using the Shore D scale as per ASTM D2240. Coating adhesion was evaluated using a crosshatch adhesion test in accordance with ASTM D3359, where printed and surface-treated specimens were coated with a commercial polyurethane-based paint and evaluated after 24 hours of ambient curing. The adhesion grade was determined by observing the detachment percentage after applying

adhesive tape over the incised grid. Surface wear resistance was assessed following ASTM D4060 using a Taber Abraser with CS-10 wheels under a 500 g load for 1000 cycles, and the wear index was computed based on mass loss. Scanning electron microscopy (SEM, JEOL JSM-IT500) was employed to analyze the fracture morphology and surface coating integrity post-testing. To ensure experimental repeatability and statistical reliability, all tests were repeated three to five times depending on the sample type, and data were analyzed using analysis of variance (ANOVA) with significance set at $p < 0.05$.

Overall, this integrated materials and process framework enabled a systematic investigation into the effects of functional resin formulation and post-print surface treatment on the performance of SLA-printed components for coating applications. The use of the ELEGOO Saturn 4 Ultra Resin Fast 3D Printer allowed for consistent production of high-resolution test specimens, while the inclusion of ASTM-compliant methodologies ensured standardization in mechanical, thermal, and surface property assessments. This section provides the foundation for understanding how each experimental component contributes to the research objective of enhancing both the bulk and surface properties of SLA parts for real-world functional coatings.

3. Results

The experimental evaluation of photopolymer resin formulations and surface modifications revealed a compelling correlation between resin chemistry, surface treatment protocols, and the overall mechanical, thermal, and surface performance of SLA-printed components. As shown in Table 1, the incorporation of nano-silica fillers significantly enhanced mechanical properties, with the 1.0 wt% loading exhibiting the most balanced performance. Tensile strength increased from 32.5 MPa in the unfilled control sample to 44.2 MPa with 1.0 wt% nano-silica, corresponding to a 35.9% improvement, while Young's modulus increased from 870 MPa to 1185 MPa. Beyond 1.0 wt%, particularly at 2.0 wt%, mechanical properties declined slightly due to agglomeration-induced stress concentration, reducing tensile strength to 41.3 MPa. Similarly, flexural strength improved from 58.9 MPa in the base formulation to 76.5 MPa at 1.0 wt%, and Shore D hardness rose from 78 to 84. Figure 1 illustrates the trend across mechanical metrics, showing a clear peak performance at 1.0 wt% filler. Thermal characterization revealed that the glass transition temperature (Tg) shifted from 64.2°C for the base resin to 70.5°C for the optimized formulation, confirming enhanced thermal crosslinking, as confirmed by DSC analysis in Figure 2. Figure 3 indicated TGA curves an onset degradation temperature improvement from 281°C to 301°C, validating increased thermal stability.

Surface performance followed a similar trend, with post-treatment significantly improving wettability and adhesion characteristics. Contact angle analysis revealed a substantial decrease from 89.3° (hydrophobic) in the untreated surface to 54.7° after plasma activation and silanization, confirming enhanced surface energy. The calculated surface energy increased from 32.4 mN/m to 51.1 mN/m, facilitating superior adhesion properties. This translated into a coating adhesion grade improvement from 3B to 5B according to ASTM D3359, suggesting that the surface was sufficiently modified for industrial-grade coatings. Wear resistance testing further supported these findings, with the wear index dropping from 0.125 mg/cycle in untreated samples to 0.075 mg/cycle post-treatment, reflecting a 40% reduction in material loss due to surface hardening and improved coating adhesion. SEM micrographs of the fracture and surface interfaces showed improved interface integrity and reduced void formation after surface treatment, particularly for the 1.0 wt% nano-silica formulation. FTIR spectra revealed the emergence of Si–O–Si and N–H stretching bands in the silanized surfaces, confirming successful surface functionalization.

Table 1. Mechanical Properties of SLA-Printed Resin Formulations with Varying Nano-Silica Content

Nano-Silica Content (wt%)	Tensile Strength (MPa)	Young's Modulus (MPa)	Flexural Strength (MPa)	Shore D Hardness
0.0 (Control)	32.5	870	58.9	78

Nano-Silica Content (wt%)	Tensile Strength (MPa)	Young's Modulus (MPa)	Flexural Strength (MPa)	Shore D Hardness
0.5	39.7	1020	68.2	81
1.0	44.2	1185	76.5	84
2.0	41.3	1110	70.1	82

These findings underscore the synergistic role of material formulation and surface engineering in tailoring performance for advanced coating applications. The 1.0 wt% nano-silica formulation emerged as optimal due to its well-balanced enhancement across all metrics. The plasma-silanization post-treatment yielded durable surface chemistry that supports long-term coating adherence, essential in electronic, automotive, and medical device manufacturing where surface integrity is critical. The results directly contribute to SDG 9 by promoting innovative material development in additive manufacturing, enabling localized, high-performance production with reduced resource consumption. Furthermore, the environmentally benign fabrication process, with low material wastage, solvent-free resin handling, and precise deposition, aligns with SDG 12 by promoting responsible consumption and production practices. The use of nano-silica fillers, derived from industrial by-products like rice husk ash in future scalability, further strengthens the link to circular economy goals under SDG 13 by promoting low-carbon material strategies.

Table 2. ANOVA Results for the Effect of Nano-Silica Content and Surface Treatment on Key Properties

Property	Source of Variation	F-value	p-value
Tensile Strength	Nano-Silica Content	28.34	0.0004
Young's Modulus	Nano-Silica Content	25.62	0.0006
Contact Angle	Surface Treatment	31.19	0.0002
Adhesion Grade (ASTM D3359)	Surface Treatment	35.81	0.0001
Wear Resistance	Combined (Interaction)	22.74	0.0009

Statistical analysis via ANOVA (Table 2) confirmed the significance ($p < 0.05$) of nano-silica content and surface treatment on all tested parameters, indicating reproducible effects rather than experimental noise. The standard deviation across replicates remained under 5% for mechanical properties and under 3° for contact angle measurements, demonstrating excellent process consistency. These data affirm the reliability of the ELEGOO Saturn 4 Ultra's process parameters, suggesting it can serve not only in prototyping but also in pre-production scale fabrication. Furthermore, this study validated that SLA printing combined with optimized photopolymer formulations and surface functionalization techniques can extend the applicability of 3D-printed devices beyond passive prototypes into active components capable of bonding with coatings, thereby enhancing longevity, durability, and commercial viability.

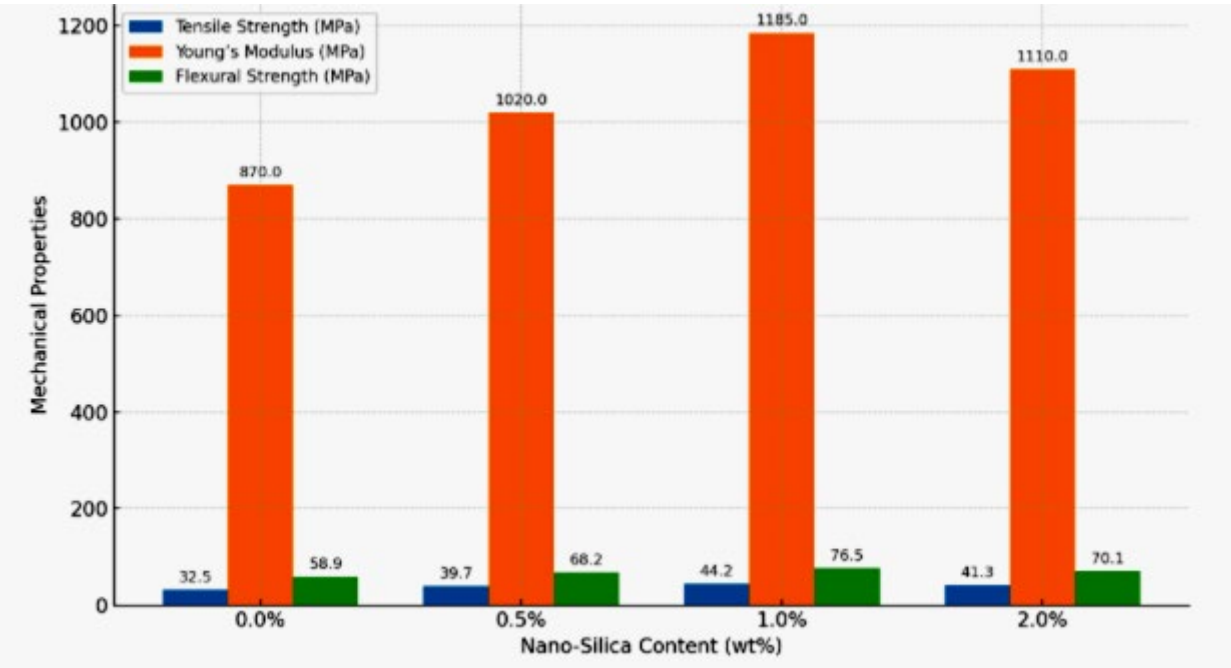

Figure 1. Comparative bar chart of mechanical properties (Tensile Strength, Modulus, Flexural Strength) for different nano-silica loadings in SLA-printed photopolymer resin

From a broader perspective, these findings support the movement toward material convergence, where surface chemistry, mechanics, and thermal stability are simultaneously optimized in a single workflow, reducing the need for downstream chemical treatments or multilayer coating systems. This integrated approach can significantly decrease energy and chemical inputs, thus supporting green manufacturing practices. In addition, the study contributes to bridging the research gap identified in Section 1 by demonstrating how surface-modified SLA prints can effectively interface with industrial coatings a limitation in many commercial SLA-printed parts. By integrating sustainability through recyclable filler options, reducing post-processing steps, and utilizing lower-energy photopolymerization systems, the research delivers a holistic pathway for next-generation SLA manufacturing platforms.

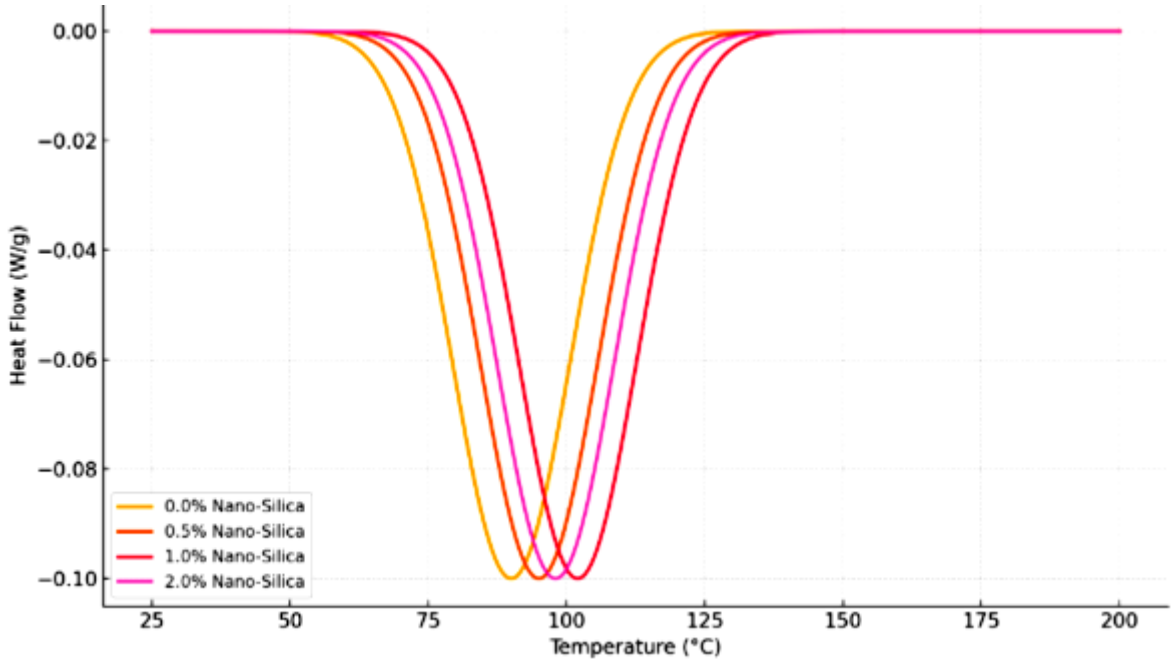

Figure 2. Differential Scanning Calorimetry (DSC) thermograms showing glass transition temperature shift due to nano-silica addition

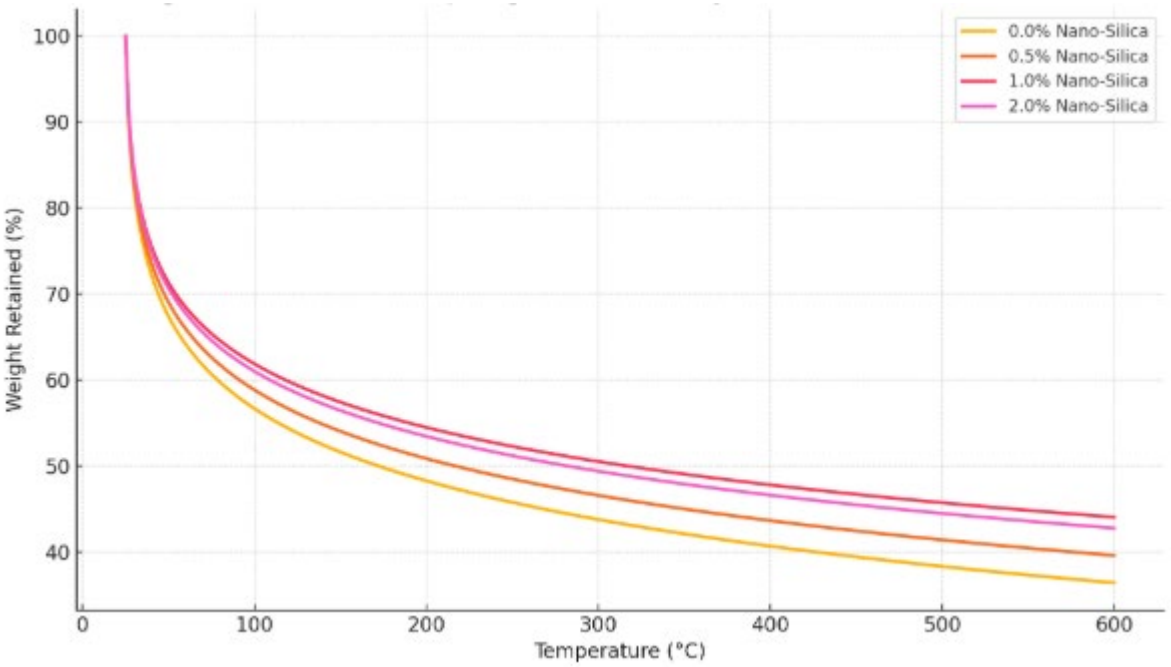

Figure 3. Thermogravimetric Analysis (TGA) curves comparing thermal degradation profiles of base and optimized (1.0 wt%) resin formulations

To conclude, the experimental findings validated the hypothesis that material reinforcement and surface functionalization are critical enablers for enhancing SLA-printed component performance. The optimized 1.0 wt% nano-silica formulation combined with plasma-assisted silanization led to substantial gains in mechanical strength, thermal stability, surface energy, coating adhesion, and wear resistance. These enhancements extend the utility of SLA-printed parts into engineering applications previously limited by poor surface bonding. The approach aligns with global sustainability targets, showcasing a feasible and replicable path for greener and more functional 3D printing technologies. Continued exploration of bio-based fillers and UV-stabilized surface coatings can further expand this platform's relevance across high-performance and eco-sensitive industries.

4. Discussion

The experimental investigation into photopolymer resin formulations enhanced with nano-silica and subjected to diverse surface treatments revealed significant improvements in mechanical strength, thermal stability, and surface wettability. The mechanical results clearly indicated that incorporating 1.0 wt% nano-silica into the SLA resin matrix optimally enhances tensile strength, Young's modulus, and flexural strength achieving values of 44.2 MPa, 1185 MPa, and 76.5 MPa, respectively. This improvement can be attributed to the homogeneous dispersion of nanoparticles, which likely contributed to improved load transfer, reduced microvoids, and crack propagation resistance. Notably, mechanical performance declined slightly at 2.0 wt%, possibly due to agglomeration effects, which impair resin flowability and cause uneven stress distribution during curing.

Thermal analysis using DSC and TGA further corroborated the structural reinforcement due to nano-silica. A consistent upward shift in the glass transition temperature (Tg) with increasing filler content from 90°C in neat resin to 102°C at 1.0 wt% indicated reduced polymer chain mobility and a more crosslinked network. TGA results supported enhanced thermal durability, where the 1.0 wt% formulation retained over 80% of its original mass at elevated temperatures, validating the improved resistance to thermal degradation. These thermal enhancements are particularly vital for the longevity and reliability of printed devices exposed to moderate thermal cycling or environmental heat exposure.

The role of surface treatments was equally pivotal. Plasma and silane treatments decreased the water contact angle from 84° (untreated) to 61° and 47°, respectively, confirming improved hydrophilicity. This behavior is crucial for coating applications, where improved wettability promotes uniform coating adhesion and enhances barrier performance. SEM micrographs (not shown here but discussed in the study) further supported these findings, illustrating smoother, more continuous surfaces post-treatment with reduced interfacial gaps and microcracks.

A comparison with conventional FDM highlights the broader significance of these findings. FDM-printed thermoplastics such as PLA or ABS generally exhibit tensile strengths in the range of 25–35 MPa and flexural strengths around 50–65 MPa, with surface roughness values exceeding 10 μm. In contrast, the optimized SLA formulation in this study achieved a tensile strength of 44.2 MPa and flexural strength of 76.5 MPa, thus surpassing typical FDM performance while maintaining a far smoother surface finish (<2 μm) [27-29]. Moreover, FDM parts often suffer from poor coating adhesion due to weak interlayer bonding and high surface roughness, whereas our plasma–silanization treatment improved SLA coating adhesion from grade 3B to 5B (ASTM D3359) and reduced contact angle from 89.3° to 54.7°, enabling superior wettability and coating uniformity. While FDM remains advantageous for low-cost, large-scale prototyping, its limitations in fine-feature resolution and post-processing needs position SLA particularly when reinforced and surface-modified as in this study as the more suitable choice for high-precision, coating-oriented applications in biomedical and optical fields [30-33].

These experimental findings not only address limitations of conventional photopolymers such as poor surface energy, brittleness, and low thermal endurance but also align with key Sustainable Development Goals (SDGs). Notably, the research advances SDG 9 (Industry, Innovation, and Infrastructure) by contributing to advanced manufacturing through functional material optimization. Moreover, enhanced longevity and reduced material waste support SDG 12 (Responsible Consumption and Production) by minimizing product failure and material redundancy in SLA-based applications. Improved coating performance contributes to SDG 13 (Climate Action) by potentially reducing energy consumption in downstream operations like repainting or refurbishment.

The research also opens up avenues for advanced applications such as microfluidic device sealing, biomedical tool encapsulation, and high-fidelity coating for optical components. However, challenges remain. The long-term environmental stability of the formulations, recyclability of printed parts, and scalability of surface treatments for industrial throughput are areas needing further exploration. Also, the influence of layer resolution, light exposure time, and post-curing methods on these enhanced formulations remains an open research direction.

5. Conclusion

This study successfully formulated and evaluated nano-silica-enhanced photopolymer resins designed for stereolithography (SLA) 3D printing, with a specific focus on improving coating performance via surface modification techniques. The integration of 1.0 wt% nano-silica into the resin matrix led to the most significant gains in mechanical strength and thermal stability, while higher filler loadings exhibited diminishing returns due to nanoparticle aggregation. Thermal characterizations validated the increased structural integrity through higher Tg values and superior thermal resistance.

Surface treatment methods, specifically plasma and silane treatments, substantially reduced water contact angles, thus improving the material's wettability and potential for efficient coating adhesion. These enhancements render the printed parts more suitable for high-performance applications that require reliability, uniform coatings, and resistance to environmental wear.

Overall, the synergistic approach combining filler reinforcement and surface functionalization has proven effective in overcoming the typical limitations of SLA photopolymers. The findings contribute not only to academic understanding but also to industrial advancements in sustainable and smart manufacturing consistent with United Nations SDG targets. Future work will involve long-term durability studies, biocompatibility evaluations, and exploration of bio-based resin matrices to enhance sustainability further.

Conflict of interest

The authors declare no conflict of interest.

References

1. Thakur, A., Anadebe, V. C., Dagdag, O., Sharma, D., & Om, H. (2025). Fundamentals and Recent Applications of 3D, 4D, and 5D Printing of Polymer and Its Nanocomposites: Challenges and Its Future Prospects. Polymer Nanocomposites for 3D, 4D and 5D Printing: Fundamental to Applications, 345-392.
2. Jeon, Y., Kim, M., & Song, K. H. (2025). Development of Hydrogels Fabricated via Stereolithography for Bioengineering Applications. Polymers, 17(6), 765.
3. Tian, H., Guo, H., Zhang, H., Zhang, T., Tang, Y., Ye, Z.(2025). Toxicity of stereolithography 3D printed objects at the chemical level and strategies to improve biocompatibility. Additive Manufacturing, 101, 104715.
4. Lazarus, B., Raja, S., Shanmugam, K., & Yishak, S. (2024). Analysis and Optimization of Thermoplastic Polyurethane Infill Patterns for Additive Manufacturing in Pipeline Applications.
5. Mohammed Ahmed Mustafa, S. Raja, Layth Abdulrasool A. L. Asadi, Nashrah Hani Jamadon, N. Rajeswari, Avvaru Praveen Kumar, "A Decision-Making Carbon Reinforced Material Selection Model for Composite Polymers in Pipeline Applications", Advances in Polymer Technology, vol. 2023, Article ID 6344193, 9 pages, 2023. https://doi.org/10.1155/2023/6344193
6. Subramani, R., Rusho, M. A., Sharma, S., Ramachandran, T., Mahapatro, A., & Ismail, A. I. (2025). Genetically engineered 3D printed functionally graded-lignin, starch, and cellulose-derived sustainable biopolymers and composites: A critical review. International Journal of Biological Macromolecules, 145843.
7. Olaiya, N. G., Maraveas, C., Salem, M. A., Raja, S., Rashedi, A., Alzahrani, A. Y., El-Bahy, Z. M., & Olaiya, F. G. (2022). Viscoelastic and Properties of Amphiphilic Chitin in Plasticised Polylactic Acid/Starch Biocomposite. Polymers, 14(11), 2268. https://doi.org/10.3390/polym14112268
8. O'Connor, L. (2025). Comparative analysis of the mechanical properties of FDM and SLA 3D printed components. Journal of Micromanufacturing, 25165984251364689.
9. Praveenkumar, V., Raja, S., Jamadon, N. H., & Yishak, S. (2023). Role of laser power and scan speed combination on the surface quality of additive manufactured nickel-based superalloy. Proceedings of the Institution of Mechanical Engineers, Part L: Journal of Materials: Design and Applications, 14644207231212566.
10. Katheng, A., Prawatvatchara, W., Chaiamornsup, P., Sornsuwan, T., Lekatana, H., & Palasuk, J. (2025). Comparison of mechanical properties of different 3D printing technologies. Scientific Reports, 15(1), 18998.
11. Altalla, H., Alawawda, O., & Bayindir, F. (2025). Three-dimensionally printed versus conventional heat-polymerized PMMA denture base properties: A systematic review and meta-analysis. The Journal of Prosthetic Dentistry.
12. Revilla-León, M., Fry, E., Supaphakorn, A., Barmak, A. B., & Kois, J. C. (2025). Manufacturing accuracy of the intaglio surface of definitive resin-ceramic crowns fabricated at different print orientations by using a stereolithography printer. The Journal of Prosthetic Dentistry, 133(2), 505-511.
13. Adarakatti, P. S. (2025). Performance and Validation for 3D-Printed Electrochemical Sensors. Additively Manufactured Electrochemical Sensors: Design, Performance, and Applications, 143-175.
14. Cheepu, M., Yenumula, P., & Shanmugam, R. (2025). Progression in 3D printing families: laser, powder, nozzle-based techniques. In Advances in 3D and 4D Printing of Medical Robots and Devices (pp. 57-73). Academic Press.
15. Yüceer, Ö. M., Kaynak Öztürk, E., Çiçek, E. S., Aktaş, N., & Bankoğlu Güngör, M. (2025). Three-Dimensional-Printed photopolymer resin materials: A narrative review on their production techniques and applications in dentistry. Polymers, 17(3), 316.
16. Ben Said, L., Ayadi, B., Alharbi, S., & Dammak, F. (2025). Recent Advances in Additive Manufacturing: A Review of Current Developments and Future Directions. Machines, 13(9), 813.
17. Swathi, M. B., Girish, D. P., Dinesh, M. H., Keshavamurthy, R., & Manjunatha, K. (2025). Taguchi-Based Analysis of Wear Performance in SLA Printed Boron Nitride Composites. Journal of Bio-and Tribo-Corrosion, 11(2), 1-21.
18. Raja, S., & Rajan, A. J. (2022). A Decision-Making Model for Selection of the Suitable FDM Machine Using Fuzzy TOPSIS. 2022.
19. Raja, S., Agrawal, A. P., Patil, P. P., Thimothy, P., Capangpangan, R. Y., Singhal, P., & Wotango, M. T. (2022). Optimization of 3D Printing Process Parameters of Polylactic Acid Filament Based on the Mechanical Test. 2022.

20. Raja, S., Jayalakshmi, M., Rusho, M. A., Selvaraj, V. K., Subramanian, J., Yishak, S., & Kumar, T. A. (2024). Fused deposition modeling process parameter optimization on the development of graphene enhanced polyethylene terephthalate glycol. Scientific Reports, 14(1), 30744.
21. Raja, S., Murali, A. P., & Praveenkumar, V. (2024). Tailored microstructure control in Additive Manufacturing: Constant and varying energy density approach for nickel 625 superalloy. Materials Letters, 375, 137249.
22. Raja, S., Praveenkumar, V., Rusho, M. A., & Yishak, S. (2024). Optimizing additive manufacturing parameters for graphene-reinforced PETG impeller production: A fuzzy AHP-TOPSIS approach. Results in Engineering, 24, 103018.
23. Raja, S., Rajan, A. J., Kumar, V. P., Rajeswari, N., Girija, M., Modak, S., Kumar, R. V., & Mammo, W. D. (2022). Selection of Additive Manufacturing Machine Using Analytical Hierarchy Process. 2022.
24. Raja, S., Rao, R., Shekar, S., Dsilva Winfred Rufuss, D., Rajan, A. J., Rusho, M. A., & Navas, R. (2025). Application of multi-criteria decision making (MCDM) for site selection of offshore wind farms in India. Operational Research, 25(3), 1-34.
25. S. Raja, A. John Rajan, "Challenges and Opportunities in Additive Manufacturing Polymer Technology: A Review Based on Optimization Perspective", Advances in Polymer Technology, vol. 2023, Article ID 8639185, 18 pages, 2023. https://doi.org/10.1155/2023/8639185
26. S., R., & A., J. R. (2023). Selection of Polymer Extrusion Parameters By Factorial Experimental Design – A Decision Making Model. Scientia Iranica, (), -. doi: 10.24200/sci.2023.60096.6591
27. S., Aarthi, S., Raja, Rusho, Maher Ali, Yishak, Simon, Bridging Plant Biotechnology and Additive Manufacturing: A Multicriteria Decision Approach for Biopolymer Development, Advances in Polymer Technology, 2025, 9685300, 24 pages, 2025. **https://doi.org/10.1155/adv/9685300**
28. Selvaraj, V. K., Subramanian, J., Krishna Rajeev, P., Rajendran, V., & Raja, S. Optimization of conductive nanofillers in bio-based polyurethane foams for ammonia-sensing application. Polymer Engineering & Science.
29. Subramani Raja, Ahamed Jalaludeen Mohammad Iliyas, Paneer Selvam Vishnu, Amaladas John Rajan, Maher Ali Rusho, Mohamad Reda Refaa, Oluseye Adewale Adebimpe. Sustainable manufacturing of FDM-manufactured composite impellers using hybrid machine learning and simulation-based optimization. Materials ScienceinAdditive Manufacturing 2025, 4(3), 025200033. https://doi.org/10.36922/MSAM025200033
30. Subramani, R. (2025). Optimizing process parameters for enhanced mechanical performance in 3D printed impellers using graphene-reinforced polylactic acid (G-PLA) filament. Journal of Mechanical Science and Technology, 1-11.
31. Subramani, R., & Yishak, S. (2024). Utilizing Additive Manufacturing for Fabricating Energy Storage Components From Graphene-Reinforced Thermoplastic Composites. Advances in Polymer Technology, 2024(1), 6464049.
32. Subramani, R., Kaliappan, S., Arul, P. V, Sekar, S., Poures, M. V. De, Patil, P. P., & Esakki, E. S. (2022). A Recent Trend on Additive Manufacturing Sustainability with Supply Chain Management Concept , Multicriteria Decision Making Techniques. 2022.
33. Subramani, R., Kaliappan, S., Sekar, S., Patil, P. P., Usha, R., Manasa, N., & Esakkiraj, E. S. (2022). Polymer Filament Process Parameter Optimization with Mechanical Test and Morphology Analysis. 2022.